ANALYSIS OF OUTPUT VOLTAGE RIPPLE FOR DUAL RANDOMIZED PWM BUCK CONVERTER OPERATING IN CONTINUOUS AND DISCONTINUOUS CONDUCTION MODES

Aimad Boudouda[a,*], Nasserdine Boudjerda[b], Fares Nafa[a]

[a] *University M'hamed Bougara, Faculty of Technology, Laboratoire Ingénierie des Systèmes et Télécommunications (LIST) , Cité Frantz. Fanon, 35000, Boumerdes, Algeria*

[b] *University of Jijel, Laboratory of Renewable Energy (LER), Jijel, Algeria*

* corresponding author: a.boudouda@univ-boumerdes.dz

ABSTRACT. Dual Randomized Pulse Width Modulation (DRPWM) is renowned for its better effectiveness than Simple Randomized Pulse Width Modulation (SRPWM) in reducing conducted Electro-Magnetic Interferences (EMI) in power converters. However, the introduction of low-frequency ripples into the output voltage by dual randomization has not yet been addressed; this effect is investigated in this paper for a buck converter operating in both the continuous conduction mode (CCM) and the discontinuous conduction mode (DCM). First, the modulating principle is presented. Then, a general analytical expression for power spectral density (PSD) of the input current is derived and validated for the proposed DRPWM scheme for both the CCM and DCM. A comparison of the PSDs of the input current for all RPWM schemes in both the CCM and DCM shows the PSD spreading effectiveness of the dual scheme as compared to simple schemes. Finally, the low-frequency output ripple is analysed using the PSD of output voltage. The results reveal that the output voltage ripple is affected by all the randomized schemes in both the CCM and the DCM. Also, the dual scheme (RCFM-RPPM) introduces the highest low-frequency voltage ripple, especially in the CCM and for low duty cycles. In DCM, the RPPM scheme gives the lowest voltage ripple, while the RCFM scheme gives the lowest voltage ripple in the CCM. The results are confirmed by both theory and simulations.

KEYWORDS: Electro-magnetic interference (EMI), dual randomization, output voltage ripple, buck converter.

1. INTRODUCTION

Nowadays, much of the electrical energy is used through power converters, typically controlled by deterministic pulse width modulation (DPWM). This technique leads to conducted and radiated EMI to other surrounding electronic devices [1]. It is, therefore, necessary for power converters to perform the required electrical functionality while complying with international electromagnetic compatibility (EMC) standards by reducing conducted and radiated emissions [2]. For this purpose, a filtering technique can be used. However, the RPWM technique is one of the most efficient and cost-effective solutions: it allows spreading the power spectrum of input current and output voltage over a wide frequency range while significantly reducing its amplitude, which is a significant EMC benefit, requiring no additional hardware [3]. Several papers regarding this new technique have been published, principally, two simple RPWM schemes with a single randomized parameter are proposed; the scheme in which the switching period is randomized (Randomized Carrier Frequency Modulation: RCFM) and the scheme in which the period is kept constant and the pulse position is randomized (Randomized Pulse Position Modulation: RPPM), for both the DC-DC [3–10] and the DC-AC [8–11]. For a maximum spreading of the voltage spectrum, a combination of the two simple schemes (RCFM and RPPM) that we call (RCFM-RPPM) or the DRPWM scheme has also been proposed [8–11]. It has been reported, in [8], that this combined scheme gives the most spread spectrum of the input current in DC-DC converters operating in DCM. However, this effect has not yet been addressed in CCM. Despite the benefits of RPWM in spreading the spectrum and reducing EMI, this technique can introduce an undesirable continuous noise within the pass-band of the low-pass filter in DC-DC converters and induce low-frequency output voltage ripples, which require larger and expensive filters [4–6, 12–15]. Although detailed investigations of the effect of simple schemes (RCFM and RPPM) on the low-frequency output voltage ripples of DC-DC converters operating in CCM and DCM are given in [3, 7], the effect of (RCFM-RPPM) on the output voltage ripples at low-frequencies has not yet been investigated.

This paper aims to investigate the effect of the DRPWM scheme on both the input current and the output voltage ripples of a buck converter operating in CCM and DCM. At first, the modulating principle of DRPWM is presented. Then, a general analytical model of the PSD valid for input and output currents is derived in both CCM and DCM. Note that the simple schemes (RCFM and RPPM) are directly deduced as particular
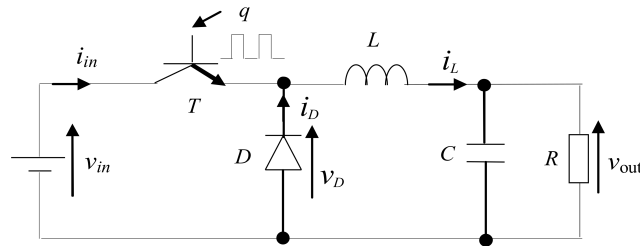
FIGURE 1. Buck converter.
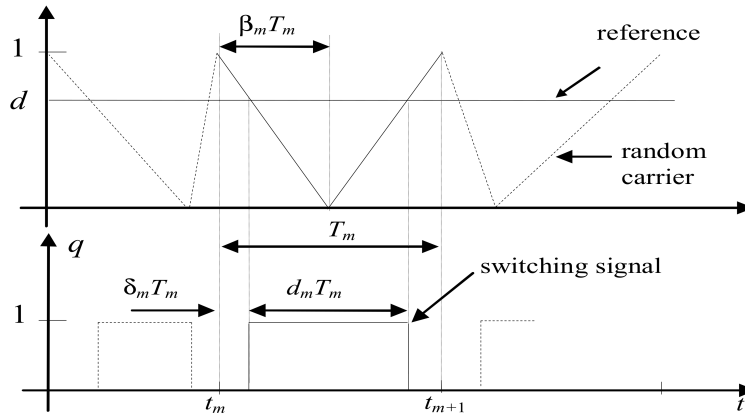
FIGURE 2. Modulating principle.

cases from the general model. The proposed analytical model is validated by a comparison to simulation results under MatLab-Simulink using the Welch estimation of the PSD, which gives satisfactory results [8, 10, 11]. A comparison between PSDs of the input current for the three schemes in both the CCM and the DCM is presented. The PSD of the output voltage ripple under each scheme is presented and compared in both conduction modes. Finally, simulation results confirm the theoretical evaluations.

2. RPWM TECHNIQUE IN BUCK CONVERTER

2.1. MODULATING PRINCIPLE

The converter under study is schematized in Figure 1; it requires one switching signal q. It can operate in CCM and DCM [3, 16–19].

For DPWM, the switching signal q is obtained by a comparison of a reference signal to a deterministic triangular carrier. In the case of RPWM, the reference signal is compared to a random triangular carrier.

The switching signal q is characterised by three parameters as shown in Figure 2: the switching cycle T, (the carrier period), the duty cycle d and the delay report δ. In DC-DC, the reference signal is fixed, which leads to a constant duty cycle d. In RPWM, these three parameters should be randomized in a combined or a separate way. In practice, d is deduced from a deterministic reference signal giving the control of the output voltage v_{out}. Thus, only the switching period T and the delay report δ can be randomized.

From Figure 2, the delay report δ_m of the switching signal q can be expressed as follows:

$$\delta_m = \beta_m(1 - d) \tag{1}$$

Note   The use of parameter β rather than δ is paramount; it allows the pulse position to be defined directly from the carrier parameter β_m.

The randomization of β in the interval $[0, 1]$ gives a random delay report δ in the interval $[0, (1 - d)]$ and the resulting position of the switching signal varies randomly from the beginning $(\delta_{min} = 0)$ to the end of the switching period $(\delta_{max} = 1 - d)$. Thus, the RPPM scheme requires a triangular carrier with a fixed period T and a randomized fall time report β.

The random carrier frequency modulation (RCFM) needs a carrier with a randomized period T between two values T_{min} and T_{max} and fixed fall time report β. The randomization limits T_{min} and T_{max} are fixed around a mean value $\overline{T}$. For the buck converter, a sawtooth with a randomized period T is usually used $(\beta = 0)$.

PWM Schemes	β	T
DPWM	fixed[a]	fixed
RPPM	randomized	fixed
RCFM	fixed[a]	randomized
RCFM-RPPM	randomized	randomized

a: $\beta = 0$

TABLE 1. Resulting RPWM schemes.
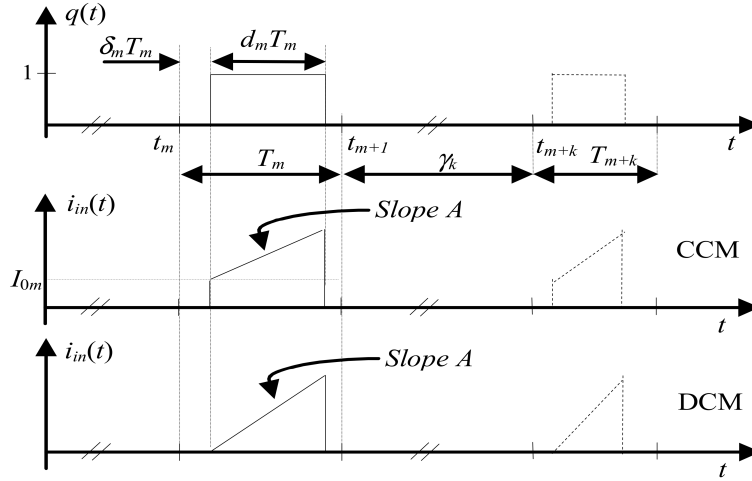
FIGURE 3. Switching signal and input current in CCM and DCM.

The proposed DRPWM combines the two previous schemes.

Related to the randomized parameters T and β, the resulting RPWM schemes are summarized in Table 1.

2.2. CONTINUOUS AND DISCONTINUOUS CONDUCTION MODE

In the buck converter, the electronic switch (MOSFET or IGBT) chops both the input current and the output voltage at high switching frequencies, resulting in high (dv/dt) and (di/dt). This will cause a high EMI and will affect nearby electronic devices [3]. The switching signal q is approximated with a square wave and the input current i_{in} can be approximated with a triangular wave in CCM and DCM, as shown in Figure 3, [3, 8].

For a switching cycle T_m, in CCM and DCM, both the input current (i_{in}) and the inductor current (i_L) can be expressed as follows:

$$i_m(t) \begin{cases} A \times (t - t_m - \delta_m T_m) + I_{0m}, & \text{for: } \delta_m T_m \leq t - t_m \leq \delta_m T_m + dT_m \\ I_m - B \times (t - t_m - \delta_m T_m - d_{T_m}), & \text{for: } \delta_m T_m + dT_m \leq t - t_m \leq \delta_m T_m + dT_m + d_1 T_m \\ 0, & \text{elsewhere.} \end{cases} \quad (2)$$

And the general expression of Fourier transform $I_m(f)$ of the current $i_m(t)$ is:

$$I_m(f) = \frac{1}{(2\pi f)^2} \left\{ [A + B + j2\pi f d_m T_m (A - F)] e^{-j2\pi f d_m T_m} \right.$$
$$\left. - [B - j2\pi f d_m T_m (F - BH)] e^{-j2\pi f (1+H) d_m T_m} + j2\pi f I_{0m} \left(e^{-j2\pi f d_m T_m} - 1 \right) - A \right\} e^{-j2\pi f \delta_m T_m} e^{-j2\pi f t_m}, \quad (3)$$

where:

t_m is the starting time of the mth switching cycle,

T_m is the mth switching cycle,

d is the mth duty cycle,

δ_m is the mth delay report: $\delta_m = \beta_m \times (1 - d)$,

I_{0m} is the initial value of the current pulse at: $t = t_m + \delta_m T_m$. Note that the value of I_{0m} is the only difference between the DCM and the CCM: For DCM, $I_{0m} = 0$ and for CCM, $I_{0m} > 0$,

I_m is the peak value of the current pulse at $t = t_m + \delta_m T_m + dT_m$, given by the relation: $I_m = FdT_m$,

Type of current	Input current (i_{in})	Inductor current (i_L)
A	$\frac{v_{in}-v_{out}}{L}$	$\frac{v_{in}-v_{out}}{L}$
B	0	$\frac{v_{out}}{L}$
F	0	$\frac{v_{in}-v_{out}}{L}$
H	$\frac{v_{in}-v_{out}}{v_{out}}$	$\frac{v_{in}-v_{out}}{v_{out}}$
v_{out}	$\frac{1}{2}\left(\sqrt{\left(\frac{K}{v_{in}}\right)^2+4K}-\frac{K}{v_{in}}\right)$	$K=\frac{(dv_{in})^2 RT}{2L}$

TABLE 2. Values of A, B, F, H and v_{out} in the buck converter.

A and B are the slopes of the rising edge and the falling edge, respectively (Table 2),

F and H are constants (Table 2).

3. Spectral analysis of input current using power spectral density

The PSD allows for a rigorous spectral analysis of random signals; it can be expressed as follows [3, 10, 20]:

$$S(f) = \lim_{\tau \to \infty} \frac{1}{\tau} E\left\{ |F[u_\tau(t)]|^2 \right\}, \tag{4}$$

where:

$u_\tau(t)$: Considered signal during the time interval τ,

$F[u_\tau(t)]$: Fourier transform of $u_\tau(t)$,

$E\{.\}$: Statistical expectation.

3.1. Analytical expression of the PSD using wiener-khinchin theorem

For a random pulse signal $i(t)$, belonging to the class of Wide Sense Stationary (WSS) signals, expression (4) leads to the general expression (5), [3–5, 8–11]:

$$S(f) = \lim_{N \to \infty} \frac{1}{\overline{T}} E\left[\sum_{k=-N}^{N} I_m(f) I^*_{m+k}(f) \right], \tag{5}$$

where:

$\overline{T}$: Statistical mean of the switching period.

$I_m(f)$ and $I^*_{m+k}(f)$ are the Fourier transforms of the signal $i_m(t)$ during the switching period T_m and its conjugate during the switching period T_{m+k}, respectively.

After some mathematical transformations, the following expression can be set as [3–5, 8–11]:

$$S(f) = \frac{1}{\overline{T}}\left\{ E_T\left[|I(f)|^2\right] + 2Real\left(\frac{E_{T,\beta}\left[I(f)e^{j2\pi fT}\right] E_{T,\beta}\left[I^*(f)\right]}{1 - E_T\left[e^{j2\pi fT}\right]} \right) \right\}, \tag{6}$$

where:

$E_T[\ ]$: Expectation related to the random variable T.

$E_{T,\beta}[\ ]$:Expectation value related to the variables T and β.

$Real(.)$: Real-part of the expression in brackets.

During the switching period T_m, Fourier transform $I_m(f)$ of the current $i_m(t)$, given by expression (2), is:

$$\begin{aligned} I(f) = \frac{1}{(2\pi f)^2} &\left\{ [A + B + j2\pi fdT(A - F)]\, e^{-j2\pi fdT} \right. \\ &\left. - [B - j2\pi fdT(F - BH)]\, e^{-j2\pi f(1+H)dT} + j2\pi fI_0\left(e^{-j2\pi fdT} - 1\right) - A \right\} e^{-j2\pi f\beta \times (1-d)T}, \end{aligned} \tag{7}$$

its conjugate form is:

$$
\begin{aligned}
I^*(f) = \frac{1}{(2\pi f)^2} & \left\{ \left[A + B - j2\pi f dT(A - F) \right] e^{j2\pi f dT} \right. \\
& \left. - \left[B + j2\pi f dT(F - BH) \right] e^{j2\pi f(1+H)dT} - j2\pi f I_0 \left(e^{j2\pi f dT} - 1 \right) - A \right\} e^{j2\pi f \beta \times (1-d)T}.
\end{aligned}
\tag{8}
$$

Notes:

- Expressions (6), (7) and (8) apply for both the input current i_{in} and the output current i_L (inductor current) by using appropriate values of constants A, B, F and H, (Table 2).

- From expressions (6), (7) and (8), the simple schemes RCFM and RPPM are deduced as particular cases: for RCFM, the parameter β is constant ($\beta = 0$) and for RPPM, the period T is constant.

3.2. WELCH APPROXIMATION OF THE PSD

To validate the analytical expressions of the PSD, the analysis of the input current is also carried out using a numerical estimation of the PSD for a representative sample of the considered signal after the simulation of the buck converter [20]. This method is very satisfactory; it gives very good results as compared to the measurement and to analytical ones [8, 10, 11]. Welch's estimation method is implemented in the Signal Processing Toolbox of MATLAB by the Pwelch function:

$$
PSD = pwelch(X, Window, Noverlap, NFFT, Fs),
$$

where,

X: Discrete-time signal vector (sampled data),

$Window$: The window function applied to segments,

$Noverlap$: The number of overlapped samples,

$NFFT$: The number of discrete FFT samples used to calculate the estimated PSD,

Fs: The sampling frequency.

3.3. RANDOMNESS LEVELS

T and β are the random parameters using the probability density function $p(T)$ and $p(\beta)$, respectively, the expected operator $E[I(f)]$ should be expressed as follows:

$$
E[I(T, \beta, f)] = \iint_{T\beta} p(T, \beta) I(T, \beta, f) dT d\beta,
\tag{9}
$$

where $p(T, \beta)$ is the probability density function (pdf) used for the randomization of T and β.

In practice, any probability density function may be applied. In our applications, the uniform law is used, as it is the simplest to implement. The lower and upper limits of random parameters T and β are defined as follows:

- RCFM scheme: Related to the limits T_{min} and T_{max} and the statistical mean $\overline{T}$, a randomness level R_T is defined as follows: $R_T = \frac{T_{max} - T_{min}}{\overline{T}}$. Thus, T varies between $T_{min} = \overline{T}\left(1 - \frac{R_T}{2}\right)$ and $T_{max} = \overline{T}\left(1 + \frac{R_T}{2}\right)$. Theoretically, the maximum randomness level is obtained using $T_{min} = 0$ and $T_{max} = 2\overline{T}$, which gives: $R_T = 2$. In practice, R_T is fixed by practical considerations; generally it does not exceed 0.5.

- RPPM scheme: In general, for the buck converter, $\beta = 0$ for both the classical deterministic modulation and RCFM. For RPPM, β is randomized between $\beta_{min} = 0$ and $\beta_{max} \leq 1$. Thus, the randomness level R_β is then taken equal to $\beta_{max}, (R_\beta = \beta_{max} - \beta_{min})$ and β is randomized in the interval $[0, R_\beta]$ and $R_\beta \leq 1$.

Note: In general, for the buck converter: $\beta_{min} = 0$ and $\beta_{max} = 1$, [10].

3.4. PSD ANALYSIS OF INPUT CURRENT

The analysis of the input current (i_{in}) is performed using the PSD of random signals. To reinforce the validity of our results, the PSD is calculated analytically using the expression (6), then compared to that estimated using the Welch algorithm. Both CCM and DCM are considered with the following conditions:

- Input voltage: $v_{in} = 15$ volts.

- Load: $(R = 47\,\Omega,\ L = 1\,\text{mH},\ C = 220\,\mu\text{F})$ for CCM.

(A) . RPPM scheme.

(B) . RCFM scheme.
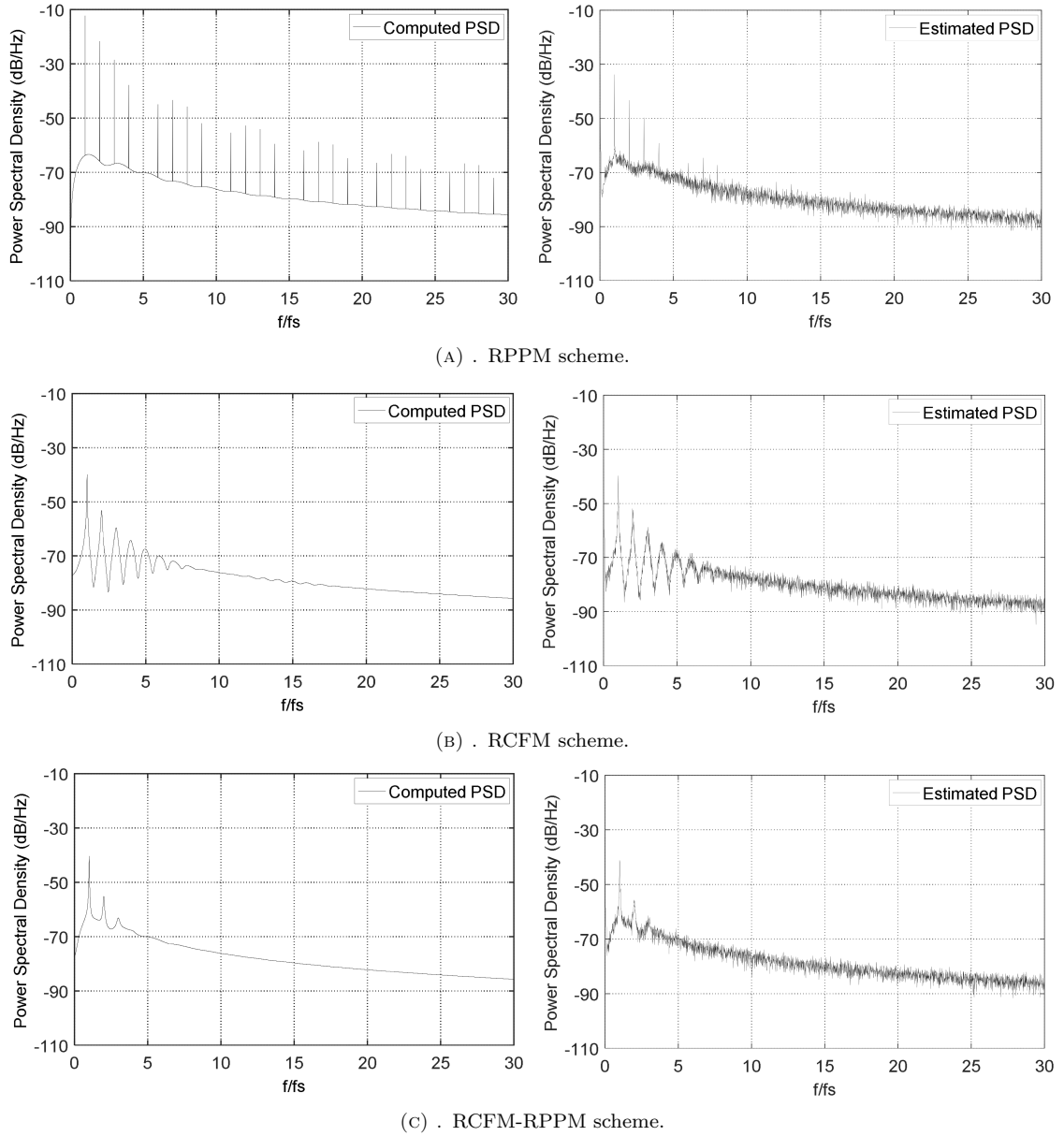
(C) . RCFM-RPPM scheme.

FIGURE 4. PSD of input current in DCM for (A) RPPM scheme, (B) RCFM scheme, (C) RCFM-RPPM scheme.

- Duty cycle: $d = 0.5$.

- Load: $(R = 47\,\Omega,\ L = 0.165\,\text{mH},\ C = 220\,\mu\text{F})$ for DCM.

- Parameters of the carrier:

  (1.) RCFM scheme: the parameter β is fixed, $(\beta = 0)$ and the period T is randomized in the interval $\left[\overline{T}\left(1 - \frac{R_T}{2}\right), \overline{T}\left(1 + \frac{R_T}{2}\right)\right], \overline{T} = \left(\frac{1}{f_s}\right), f_s = 20\,\text{kHz}$ and $R_T = 0.2$.

  (2.) RPPM scheme: T is fixed and β is randomized in the interval $[0, R_\beta]$, with $\beta_{min} = 0$ and $\beta_{max} = 0.4$, which gives $\delta_{min} = 0$ and $\delta_{max} = 0.2$.

  (3.) RCFM-RPPM scheme combines the two previous schemes (RCFM and RPPM) with the same parameters.

3.4.1. CASE OF DISCONTINUOUS CONDUCTION MODE

Figure (4a)–(4c) reveals perfect agreements between the computed PSDs using the proposed model (expression 6) and the estimated PSDs (Welch method) for RPPM, RCFM and RCFM-RPPM, respectively thereby validating our proposed model.

From Figure 4a, the RPPM scheme is not able to completely spread the PSD, which contains a continuous part (noise) and a discrete one (power harmonics), RCFM gives a completely spread PSD that considerably

(A) . RPPM scheme.

(B) . RCFM scheme.
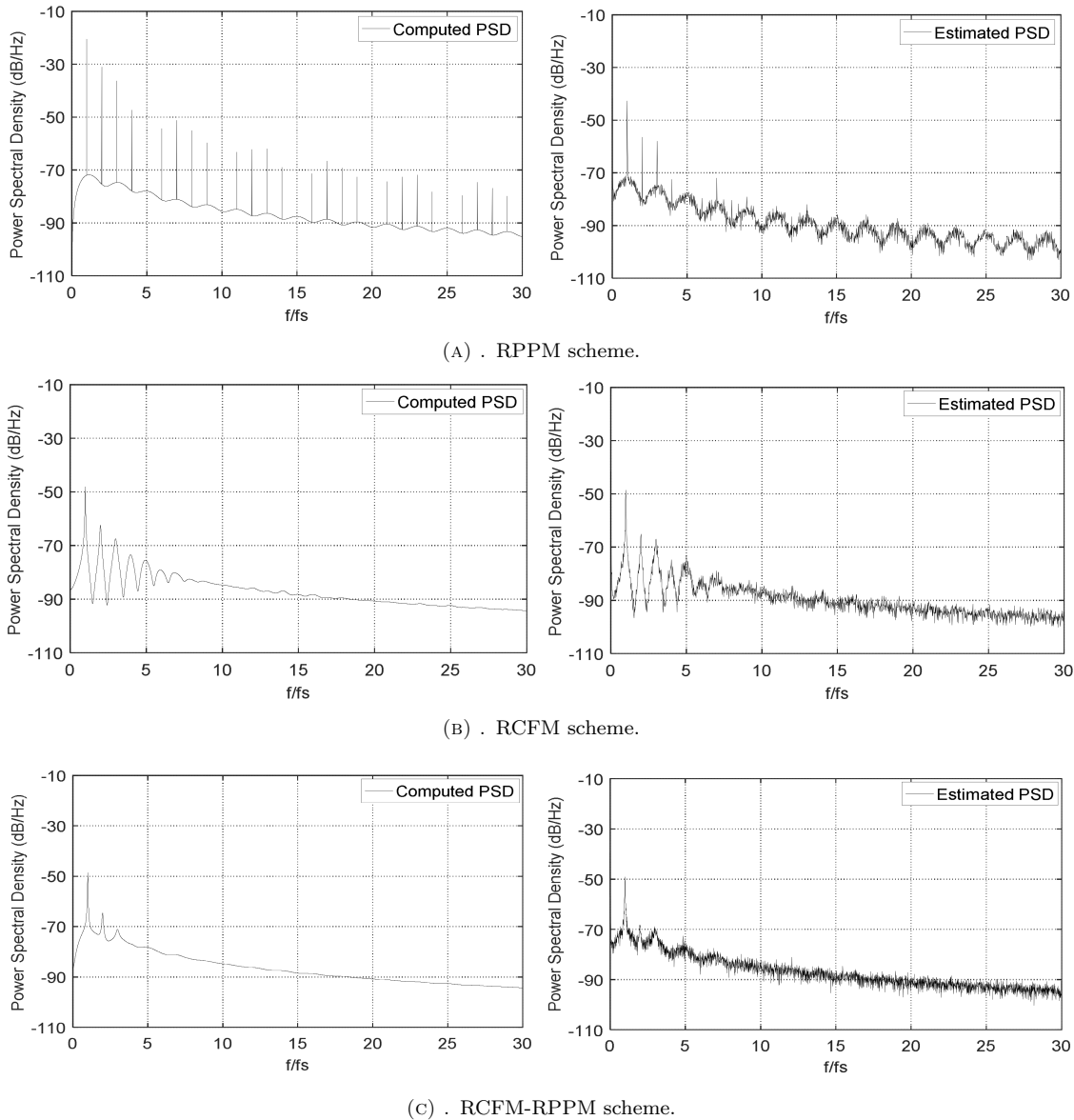
(C) . RCFM-RPPM scheme.

FIGURE 5. PSD of input current in CCM for (a) RPPM scheme, (b) RCFM scheme, (c) RCFM-RPPM scheme.

reduces the amplitude of the peaks as can be seen in Figure 4b, thus, the RCFM provides more EMC advantages than RPPM. Figure 4c clearly shows that the proposed DRPWM is the most effective in spreading the PSD and reducing its peaks; the PSD is more spread with only a meaningful peak at the switching frequency f_s; this advantage is expected because this scheme combines the properties of the two simple ones (RCFM and RPPM).

3.4.2. CASE OF CONTINUOUS CONDUCTION MODE

Figure 5a–5c compares computed and estimated PSDs for the three schemes (RPPM, RCFM and RCFM-RPPM), in CCM. A perfect agreement between the analytical model and the estimation is obtained for all schemes. In addition, the DRPWM scheme allows the most spread PSD, which is the purpose of the RPWM technique.

A comparison between Figure 4 (DCM) and Figure 5 (CCM) reveals similar shapes of the PSDs for each scheme with a lower amplitude for the CCM; this is predictable and will be discussed in the next section.

3.5. COMPARISON BETWEEN PSDS FOR CCM AND DCM

Figure 6 shows the PSD of the input current for the three schemes (RPPM, RCFM and RCFM-RPPM) and for both CCM and DCM. The PSD retains the same shape for the two modes (CCM and DCM). However, the CCM allows a significant reduction in amplitude as compared to the DCM. This is predictable because the CCM is obtained by increasing the inductance L, synonymous with reducing the current ripple (ΔI). Note that as the inductance L raises as smoothly as the input current waveform, as shown in Figure 3.

(A) . RPPM ($R\beta = 0.6$) *(the peaks are intentionally shifted to see their amplitudes).*

(B) . RCFM ($R_T = 0.2$).

(C) . RCFM-RPPM ($R_T = 0.2$, $R\beta = 0.6$).
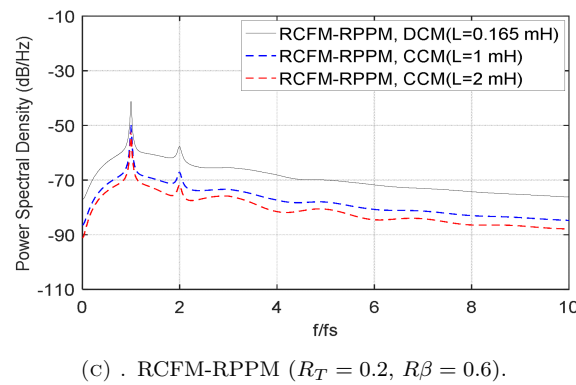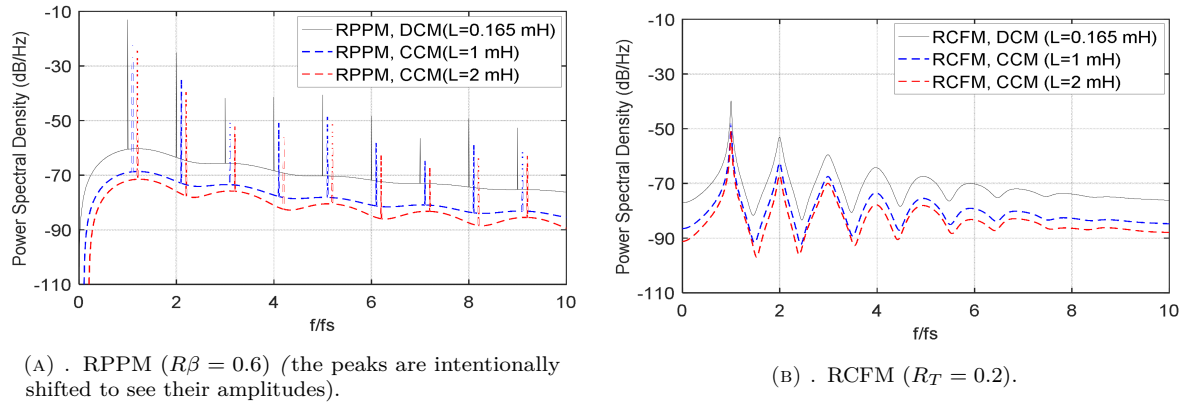
FIGURE 6. PSD of input current in DCM and CCM.
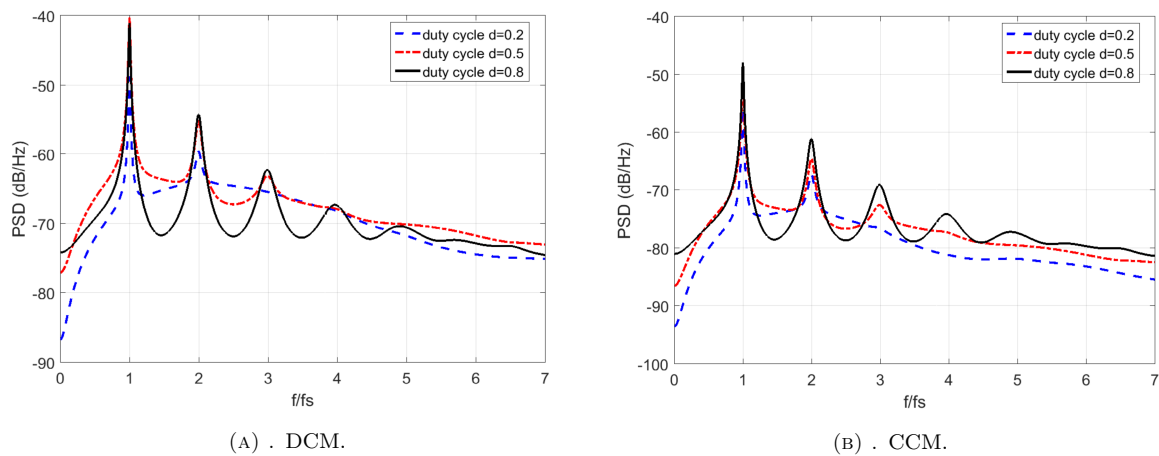
(A) . DCM.

(B) . CCM.

FIGURE 7. PSD of input current for different duty cycles: (A) DCM ($L = 0.165\,\mathrm{mH}$), (B) CCM ($L = 1\,\mathrm{mH}$).

3.6. EFFECT OF DUTY CYCLE ON THE PSD FOR CCM AND DCM

Figure 7 shows the PSDs of the input current of the buck converter in DCM and CCM, respectively, with three values of the duty cycle d: ($d = 0.2, d = 0.5$ and $d = 0.8$). The PSDs are given for the RCFM-RPPM scheme, since it gives the best spread spectrum as compared to other schemes (RPPM and RCFM).

It is obvious that the low duty cycles ($d \leq 0.5$) allow a good spread of the PSD as compared to high duty cycles ($d \geq 0.5$) in both the DCM and the CCM. This is predictable because for low duty cycles, the switching signal duration is shorter than that for high duty cycles (Figure 3) thus the randomisation of the pulse position (RPPM) has a greater effect since it is achieved in the whole switching period.

4. ANALYSIS OF OUTPUT VOLTAGE RIPPLE

The ripple value of the inductor and capacitor is another converter design parameter and one of the main design factors, which must be considered during the converter design. In our case, we focused on the analysis of the
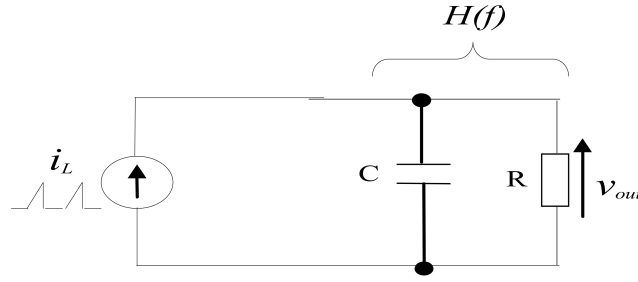
FIGURE 8. Equivalent circuit of the buck converter.

(A) . DCM.

(B) . CCM.
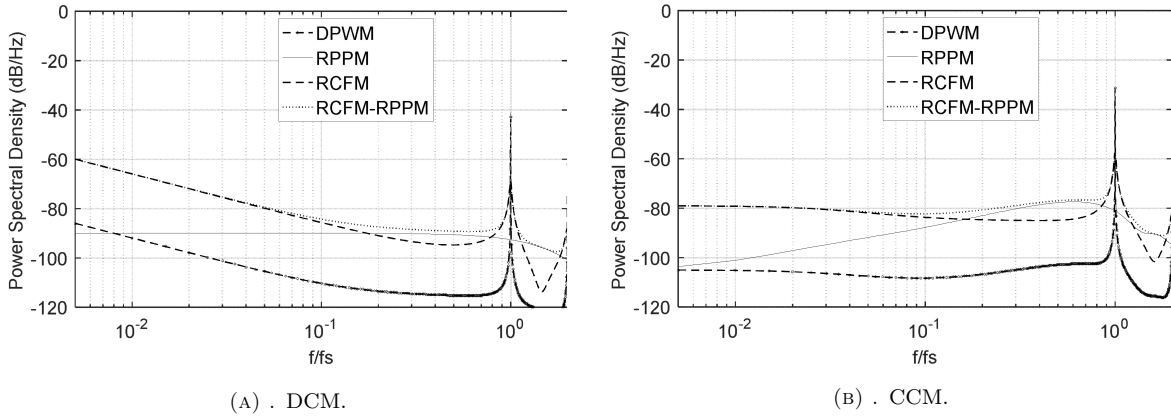
FIGURE 9. Low-frequency characterizations of v_{out}.

low-frequency ripples introduced into the output voltage by the RPWM in CCM and DCM. Then, the values of the inductor are chosen based on the conduction mode: $L = 1\,\text{mH}$ for the CCM and $L = 0.165\,\text{mH}$ for the DCM. The capacitor is fixed for the two modes ($C = 220\,\mu\text{F}$).

Note that our aim is to study the effect of the RPWM on the output voltage regardless of the filter parameters, for this reason, the inductor and capacitor values are maintained fixed for each conduction mode.

4.1. PSD OF THE LOW-FREQUENCY OUTPUT RIPPLE

As shown in Figure 8, the buck converter can be considered as a low-pass filter fed by a current source (inductor current i_L), [3, 4].

The PSD $S_{n0}(f)$ of the voltage noise at the converter output is [3]:

$$S_{n0}(f) = S_{i_L}(f)|H(f)|^2, \qquad f \neq 0, \tag{10}$$

where:

$S_{i_L}(f)$: PSD of the inductor current given by expressions (6), (7) and (8) with the corresponding values of constants A, B, F and H, (Table 2),

$H(f)$: Transfer function of the (R-C) filter given by:

$$H(f) = \frac{V_{out}(f)}{I_L(f)} = \frac{R}{1 + j2\pi fCR}. \tag{11}$$

The low-frequency characterisations of the output voltage v_{out} within the pass-band of the filter in DCM and CCM are shown in Figure 9, where the DPWM scheme is taken as a benchmark. In DCM, the RPPM introduces the lowest PSD of the output voltage, while the RCFM-RPPM introduces the highest one as shown in Figure 9a. In CCM, the RCFM introduces the lowest PSD as shown in Figure 9b, while the RCFM-RPPM always introduces the highest one.

From the previous observations, we can say that although the RCFM-RPPM gives the most spread spectrum of the input current, it introduces the largest low-frequency PSD of the output voltage in both the DCM and the CCM.

(A) . RPPM.

(B) . RCFM.
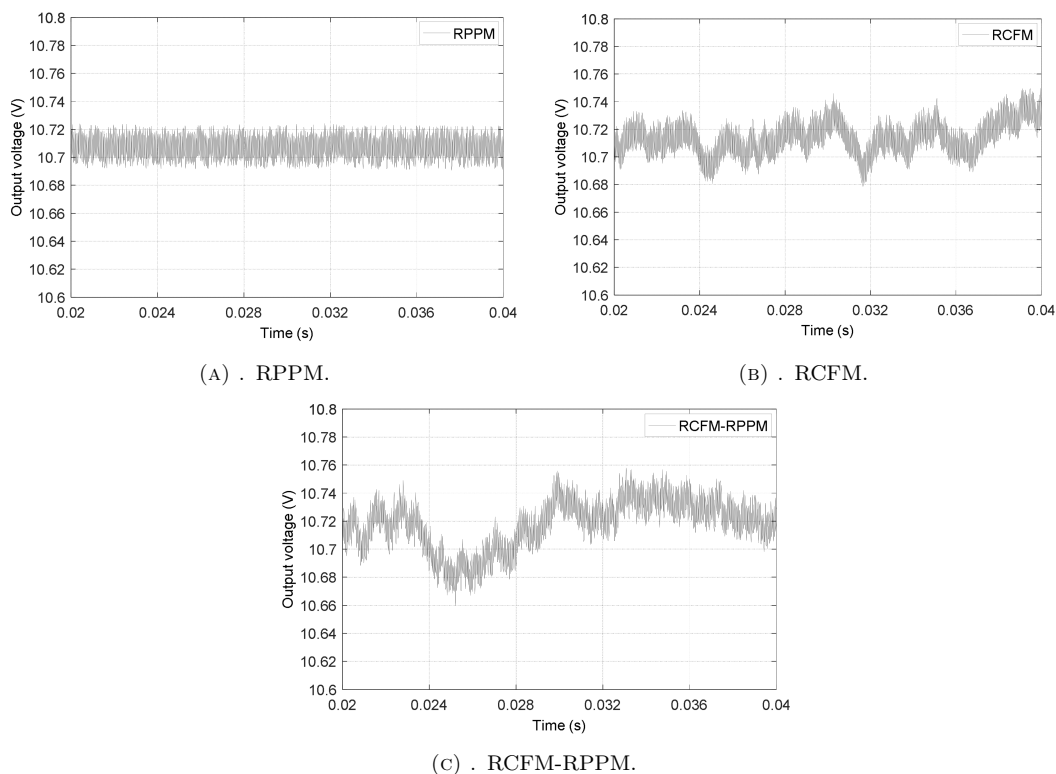
(C) . RCFM-RPPM.

FIGURE 10. Simulated output voltage ripple in DCM.

Duty cycle	Conduction mode	RPPM	ΔV	RCFM	ΔV	RCFM-RPPM	ΔV
0.2	CCM	12.08	0.16	12.04	0.08	12.07	0.13
	DCM	12.7	0.05	12.71	0.07	12.71	0.08
0.5	CCM	10.8	0.31	10.6	0.18	10.84	0.29
	DCM	10.72	0.03	10.76	0.08	10.75	0.09
0.8	CCM	6.12	0.035	6.012	0.016	6.125	0.035
	DCM	6.16	0.03	6.186	0.05	6.184	0.06

TABLE 3. Maximum peak voltage and peak-to-peak voltage ΔV.

Due to the buck converter output low pass LC filter characteristics, the low frequency ripples are considered as a significant problem, because they can easily corrupt the operation of electronic circuits [18]. The switching ripples are attenuated by the LC filter.

4.2. ANALYSIS OF THE OUTPUT RIPPLE IN DCM AND CCM

Figures 10 and 11 show the simulated output voltage waveforms for the three schemes (RPPM, RCFM and RCFM-RPPM) in DCM and CCM, respectively.

From Figure 10 and Figure 11, in Table 3, we show the maximum peak voltage and peak-to-peak voltage for all RPWM schemes, in both the DCM and the CCM. The results are given for different values of the duty cycle d.

The results of Figure 10, Figure 11 and Table 3 show a perfect agreement with those of Figure 9. Indeed, in DCM, the RPPM scheme gives the lowest voltage ripple with a magnitude of 10.72 V as shown in Figure 10 and Table 3, while the RCFM-RPPM scheme gives the highest voltage ripple with a magnitude of 10.75 V, (Table 3). In CCM, it is the RCFM scheme that gives the lowest ripple voltage with a magnitude of 10.76 V as shown in Figure 10, while the RCFM-RPPM scheme still gives the highest ripple with a magnitude of 10.84 V, (Table 3), thus confirming the theoretical prediction of Figure 9. For low duty cycles ($d \leq 0.5$), the different schemes give the highest ripple as compared to high duty cycles ($d \geq 0.5$) for both conduction modes (Table 3).

(A) . RPPM.

(B) . RCFM.

(C) . RCFM-RPPM.
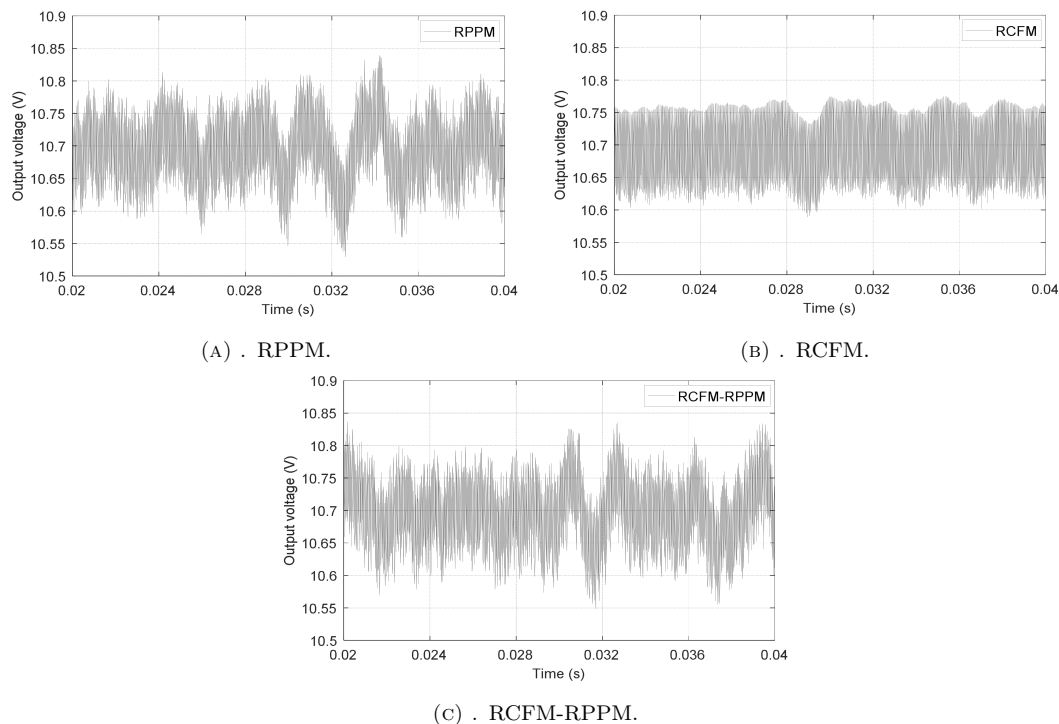
FIGURE 11. Simulated output voltage ripple in CCM.

5. CONCLUSION

This paper gives an analysis of the effect of DRPWM on the input current and the output voltage ripple of a buck converter operating in CCM and DCM. For a rigorous analysis of the current and the voltage, we have proposed and validated a general mathematical model of the PSD in CCM and DCM. Overall, the CCM mode allows a significant reduction in the PSD amplitude of the input current as compared to the DCM mode. The RCFM-RPPM scheme realizes the most effective spreading of the PSD as compared to the simple schemes (RCFM and RPPM), particularly in CCM. However, this scheme introduces the highest low-frequency voltage ripple, especially in CCM and for low duty cycles, which must be taken into consideration. The RPPM and RCFM schemes give the lowest voltage ripple in DCM and CCM, respectively, which further decreases as the duty cycle "d" increases. Finally, simulation results confirm and validate the theoretical predictions.

REFERENCES

[1] M. Miloudi, A. Bendaoud, H. Miloudi. Common and differential modes of conducted electromagnetic interference in switching power converters. *Revue Roumaine des Sciences Techniques – Serie Électrotechnique et Énergetique* **62**(3):246–251, 2017.

[2] P. Lezynski. Random modulation in inverters with respect to electromagnetic compatibility and power quality. *IEEE Journal of Emerging and Selected Topics in Power Electronics* **6**(2):782–790, 2018. https://doi.org/10.1109/JESTPE.2017.2787599.

[3] K. K. Tse, H. Shu-Hung Chung, S. Y. R. Hui, H. C. So. Spectral characteristics of randomly switched PWM DC/DC converters operating in discontinuous conduction mode. *IEEE Transactions on Industrial Electronics* **47**(4):759–769, 2000. https://doi.org/10.1109/41.857956.

[4] Y. Shrivastava, S. Y. Hui, S. Sathiakumar, et al. Harmonic analysis of nondeterministic switching methods for DC-DC power converters. *IEEE Transactions on Circuits and Systems I: Fundamental Theory and Applications* **47**(6):868–884, 2000. https://doi.org/10.1109/81.852940.

[5] V. Adrian, J. S. Chang, B.-H. Gwee. A randomized wrapped-around pulse position modulation scheme for DC–DC converters. *IEEE Transactions on Circuits and Systems I: Regular Papers* **57**(9):2320–2333, 2010. https://doi.org/10.1109/TCSI.2010.2043997.

[6] H. Guo, Z. Li, B. Zhang. Characteristic analysis of switching voltage power spectra under the mode of random carrier-frequency modulation. *COMPEL – The International Journal for Computation and Mathematics in Electrical and Electronic Engineering* **29**(2):484–494, 2010. https://doi.org/10.1108/03321641011014940.

[7] E. N. Y. Ho, P. K. T. Mok. Design of PWM ramp signal in voltage-mode CCM random switching frequency buck converter for conductive EMI reduction. *IEEE Transactions on Circuits and Systems I: Regular Papers* **60**(2):505–515, 2013. https://doi.org/10.1109/TCSI.2012.2215796.

[8] A. Boudouda, N. Boudjerda, A. Bouzida, A. Aibeche. Dual randomized pulse width modulation technique for buck converter fed by photovoltaic source. *Revue Roumaine des Sciences Techniques – Serie Électrotechnique et Énergetique* **63**(3):289–294, 2018.

[9] K. El Khamlichi Drissi, P. C. K. Luk, B. Wang, J. Fontaine. A novel dual-randomization PWM scheme for power converters. In *IEEE 34th Annual Conference on Power Electronics Specialist, 2003. PESC '03*. 2003. `https://doi.org/10.1109/PESC.2003.1218102`.

[10] A. Boudouda, N. Boudjerda, K. El Khamlichi Drissi, K. Kerroum. Spread spectrum in full bridge DC-DC/DC-AC converter by optimized dual RPWM scheme. *The Mediterranean journal of electronics and communications* **10**(1):666–673, 2014.

[11] N. Boudjerda, A. Boudouda, M. Melit, et al. Spread spectrum in three-phase inverter by an optimised dual randomised PWM technique. *International Journal of Electronics* **101**(3):308–324, 2014. `https://doi.org/10.1080/00207217.2013.780299`.

[12] Y. Shrivastava, S. Y. R. Hui, S. Sathiakumar, et al. Effects of continuous noise in randomised switching DC-DC converters. *Electronics Letters* **33**(11):919–921, 1997. `https://doi.org/10.1049/EL:19970655`.

[13] K. Cui, V. Adrian, Y. Sun, et al. A low-harmonics low-noise randomized modulation scheme for multi-phase DC-DC converters. In *2017 15th IEEE International New Circuits and Systems Conference (NEWCAS)*. 2017. `https://doi.org/10.1109/NEWCAS.2017.8010131`.

[14] K. Cui, V. Adrian, B.-H. Gwee, J. S. Chang. A noise-shaped randomized modulation for switched-mode DC-DC converters. *IEEE Transactions on Circuits and Systems I: Regular Papers* **65**(1):394–405, 2018. `https://doi.org/10.1109/TCSI.2017.2719700`.

[15] V. Nguyen, H. Huynh, S. Kim, H. Song. Active EMI reduction using chaotic modulation in a buck converter with relaxed output LC filter. *Electronics (Basel)* **7**(10):254, 2018. `https://doi.org/10.3390/electronics7100254`.

[16] E. Babaei, H. M. Mahery. Mathematical modeling and analysis of transient and steady states of buck dc-dc converter in DCM. *COMPEL – The International Journal for Computation and Mathematics in Electrical and Electronic Engineering* **32**(1):337–363, 2013. `https://doi.org/10.1108/03321641311293920`.

[17] D. Stepins. Analysis of output voltage of switching frequency modulated DC-DC converter operating in discontinuous conduction mode. In *2010 IEEE International Symposium on Industrial Electronics*. 2010. `https://doi.org/10.1109/ISIE.2010.5637199`.

[18] D. Stepins, J. Jankovskis. Reduction of output voltage ripples in frequency modulated power converter. *Elektronika ir elektrotechnika* **119**(3), 2012. `https://doi.org/10.5755/j01.eee.119.3.1361`.

[19] A. Boudouda, A. Bouzida, F. Nafa. Spectral analysis of switch voltage for dual randomized PWM DC-DC converters operating in DCM. *International Journal of Electronics Letters* **10**(1):101–114, 2022. `https://doi.org/10.1080/21681724.2020.1870717`.

[20] P. Welch. The use of fast Fourier transform for the estimation of power spectra: A method based on time averaging over short, modified periodograms. *EEE Transactions on Audio and Electroacoustics* **15**(2):70–73, 1967. `https://doi.org/10.1109/TAU.1967.1161901`.